Raman signature modification induced by copper nanoparticles in silicate glass

Philippe Colomban, Henry D. Screiber

Journal of Raman Spectroscopy 36 [9] (2005) 884-890

Comparisons were drawn from Raman analyses of alkali borosilicate glasses coloured by copper as "blue" Cu^{2+} (peak absorption at 750 nm), as "colourless" Cu^{+}, and as "opaque red" Cu^{0} (peak absorptions at ~420 and 570 nm). These glasses are good models for the understanding of the Raman signature of lustre ceramics and lustre-painted glasses. Convenient choice of the excitation wavelength provides information on the Cu° moieties environment. The silicate network around a copper nanocrystal, $(Cu^{0})_{n}$, in a glass is less polymerized than the main framework that hosts a copper ion, whether Cu^{2+} or Cu^{+}.

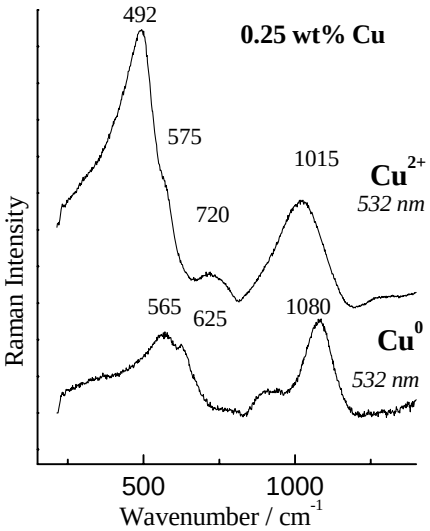

Philippe Colomban and
Henry D. Schreiber

Raman signature modification induced by copper nanoparticles in silicate glass

Raman signature modification induced by copper nanoparticles in silicate glass

Philippe Colomban[1*] and Henry D. Schreiber[2]

[1]Nanophases and Heterogenous Materials Group
LADIR, UMR7075 CNRS & Université Pierre et Marie Curie
2 rue Henry-Dunant F-94320 Thiais, France

[2]Chemistry Department, Virginia Military Institute, Lexington, VA 24450, USA

ABSTRACT

Composite materials formed by metal nanoclusters embedded in glasses/glazes have been produced for centuries (Roman *hematinum* and Renaissance *alassonti*, Coptic lustre-painted glass and Islamic lustre ceramics). Comparisons were drawn from Raman analyses of alkali borosilicate glasses coloured by copper as "blue" Cu^{2+} (peak absorption at 750 nm), as "colourless" Cu^{+}, and as "opaque red" Cu^{0} (peak absorptions at ~420 and 570 nm). In particular, Raman analyses of copper-ruby glasses containing Cu^{0} nanocrystals were performed under blue (488 nm), green (514.5 and 532 nm), and red (647.1 nm) excitations, providing information on the glass structure around the Cu^{0} precipitate. Addition of europium to Cu^{0}-containing glass melts yielded glasses that were dichroic; for example, a glass with 0.2 wt% Cu and 0.4 wt% Eu was red in absorbed light and blue in transmitted light. The backscattering Raman signature of the glassy silicate matrix containing copper indicated a less-polymerized network around the Cu^{0} nanocrystals/atoms than around Cu^{2+} or Cu^{+} (Raman index of polymerisation ~1 instead of ~2). Strong Rayleigh scattering is measured under blue excitation for all copper-containing glasses and under red excitation for Cu^{0}-containing (red) glass.

Keywords : glass, nanocrystals, metal, copper, archaeometry, lustre

*** Correspondence : philippe.colomban@glvt-cnrs.fr**
Fax 33 1 4978 1118

1. INTRODUCTION

Composite materials formed by semiconductors or metal nanoclusters embedded in glasses have been produced for centuries. For example, the famous Lycurgus 4th century Roman cup, now at the British Museum, is ruby red when viewed in transmitted light, but green in reflected light. This unique colouring is attributed to nanocrystals of a Au/Ag alloy dispersed throughout the glassy matrix [1,2]. *Hematinum* red glass cups were first described by the Roman historian Pline and Buonarotti, the famous architect and potter of Medici Dukes, who reported that the colour of *alassonti* vases changes with the observation angle [3]. The origin of glass staining dates back to the pre-Islamic, Roman period in Egypt before they were applied to a surface using heat in a furnace. The technique of heating of silver-based pigments is assigned to Coptic glassmakers in Egypt (and also to Syrian glassmakers ?) in the sixth or seven century [4]. Incorporation of elemental Ag at the glass surface remains a usual way to obtained yellow coloured stained glass windows from Middle-age – Renaissance to present time [3]. Similarly, the polychrome lustre décor on ceramics, an innovation of the Abbasid potters and the oldest nanotechnology optical device, relies on a dispersion of metallic Ag and Cu nanoparticles [5-11]. Layers are formed from colloidal Ag^0/Cu^0 nanocrystals in the near-surface region of a tin-containing lead silicate glaze, giving rise to an iridescent multicoloured reflective decoration. Recent studies [6-11] have demonstrated that the presence of Ag^0 and Cu^0 nanoparticles array is responsible for the phenomenon. But these same studies have also shown the complexities, with a large part of Cu and Ag atoms being oxidised to coloured ions and with a stacking of many metallic nanocrystal-containing layers acting as selective filters. Such layering has also been observed in the Uraniidae butterfly wing [12], in which a range of coloured scales sizes and spacings contributes to the variety of colour and iridescence.

Contemporary commercial glassmakers still employ colloidal metallic dispersions of gold, silver, and copper to generate desired colours in decorative glasses. Further, micro- and nano-structured films containing particles of elements such as Fe, Cu, and Co in both their metal and oxidised states have been proposed as promising materials for use in optoelectronics for catalysis, solar energy conversion, sensor, microwave, magnetic, and non-linear devices [13-18].

As a non-destructive technique, Raman spectroscopy has proven its potential in the analysis of the structure of amorphous silicates [19-22]. Raman spectra of luster pottery have demonstrated changes with the exciting laser wavelength in a complex fashion [7]. Raman analysis of well-characterized glasses containing copper preferentially stabilized in the Cu^{2+}, Cu^{+}, and Cu^0 states should be an initial step in the understanding of the Raman signature of luster glass and glaze. Furthermore, the Raman analysis of samples containing europium in addition to copper could give information regarding the change induced by an element favoring the reduction of copper to Cu^0 as does tin in ancient luster.

2. EXPERIMENTAL METHODS

2.1. Composition

The base composition was an alkali borosilicate glass, previously identified as SRL-131 [23]. Even though SRL-131 was initially developed as a model composition for glasses to be used in nuclear waste immobilization, its redox chemistry has been shown to be equally applicable to a wide range of commercial glasses [23]. Prescribed amounts of ultrapure oxides and carbonates

were mechanically mixed, melted in platinum crucibles, rapidly quenched, and powdered to yield a homogeneous glass frit with a nominal composition (wt%): 57.9 SiO_2, 1.0 TiO_2, 0.5 ZrO_2, 14.7 B_2O_3, 0.5 La_2O_3, 2.0 MgO, 17.7 Na_2O, and 5.7 Li_2O.

Copper, initially introduced as ultrapure CuO, was added to produce glasses with either 0.20 wt% or 0.25 wt% Cu in SRL-131. Glasses containing both copper and europium were prepared with 0.20 wt% Cu and either 0.10 wt% Eu or 0.40 wt% Eu.

2.2. Synthesis

Individual copper-containing samples were synthesized at 1150°C for at least 24 hours in a controlled-atmosphere furnace. After processing, the melts were quenched by removal from the furnace. The Cu^{2+}-Cu^{+} and Cu^{+}-Cu^{0} redox equilibria in SRL-131 at 1150°C were previously calibrated to the prevailing atmosphere during sample synthesis [24, 25]. Oxidized samples were contained within platinum capsules and were prepared in air ($fO_2 = 10^{-0.7}$ atm); such samples stabilized 40% of its copper as Cu^{2+} and 60% as Cu^{+}. Samples prepared under intermediate redox conditions (CO_2/CO gas flow ratio of 7, $fO_2 = 10^{-9.6}$ atm) were made in alumina crucibles; essentially 100% of all copper existed as Cu^{+} in these samples. Reduced samples were contained within graphite crucibles and were prepared in an atmosphere of pure CO ($fO_2 = 10^{-14.5}$ atm); such samples stabilized 70% of its copper as Cu^{0} and 30% as Cu^{+}. These reduced glasses possessed the characteristic red color of colloidal copper without further heat treatment.

The samples containing both copper and europium were prepared in the same fashion as the reduced copper-containing glasses. According to the electromotive force series established for redox couples in SRL-131 [24], europium as Eu^{2+} should act as a reducing agent to Cu^{+}, enhancing the red color of the samples.

2.3. Analysis

Polished sections about 2 mm in diameter and about 1 mm thick were prepared of the individual glasses.

Visible Absorption

Absorbance spectra were measured with a UV/vis/NIR spectrophotometer (Shimadzu UV-3100) operating between 300 and 800 nm. All spectral absorptions were normalized to a sample thickness of exactly 1.00 mm.

Raman Scattering

A multichannel notch-filtered INFINITY spectrograph (Jobin-Yvon–Horiba SAS, Longjumeau, France) equipped with a Peltier cooled CCD matrix and an "XY" spectrograph (Dilor, Lille, France) equipped with a double monochromator filter and a back-illuminated, liquid nitrogen-cooled, 2000 x 256 pixels CCD detector (Spex, Jobin-Yvon–Horiba Company) were used to record Raman spectra between 10 (XY instrument)/150 (INFINITY instrument) and 4000 cm^{-1}, using 488, 514.5, 532, and 647.1 nm exciting lines (Ar^{+}-Kr^{+}, YAG, and He-Ne lasers). The power of illumination ranged between 1 mW (INFINITY instrument, red samples) and 80 mW (XY instrument, colourless samples) as a function of the sample colour, instrument, and wavelength. Backscattering illumination and collection of the scattered light were made through an Olympus confocal microscope (long focus Olympus x10 or x50 objective, total magnification x100 or x500).

2.3. Peak fitting

In undertaking a curve fit of the Raman spectra, the segment linear baseline was first subtracted using Labspec (Dilor) software. The number of reference points was minimal, from 4 to 8, and was kept constant for attaching the baseline segment to the different spectra. A gaussian shape was assumed for most Raman lines of the glassy silicate network because of the amorphous state of examined materials; a lorentzian shape is used for narrow components related to crystalline moieties and electronic transitions. The same spectral windows were used for the extraction of the components using the Origin software peak-fitting module (Microcal Software, Inc.). The integral area under each component of the envelope was calculated. The following assumptions were made: i) for the Si-O stretching range (see further) extending from 700 to 1300 cm^{-1} we postulated 4(/5) components assigned to Q_0, Q_1, Q_2 and Q_3(/Q_4), no separation being possible between the two latter components [7,21-22], and ii) we postulated rather similar bandwidths; for the Si-O bending range, the number of bands is also 4 or less.

3. RESULTS

3.1. Colour and Visible Absorption

Figure 1 compares the visible absorption spectra for glasses with the same total copper content (0.25 wt% Cu) but equilibrated at different oxygen fugacities. The reduced glass is an opaque red colour attributed to Cu^0 nanocrystals, $(Cu^0)_n$ [26]. Its spectrum shows a rather narrow peak at about 570 nm; the narrow peak is characteristic of a colloidal dispersion of metallic nanocrystals in glass [1]. A broader spectral contribution is centered around 430 nm, usually correlated with isolated Cu^0 atoms in the glass. Consequently, the 532 and 514.5 nm exciting lines (of the Raman scattering excitation laser line) should interact with the $(Cu^0)_n$ chromophore associated with the narrow peak, and the blue excitation line with both Cu^0 species. The Cu^+-containing glass is colorless; consequently, it shows no unique absorbances in the 400 – 800 nm spectral region. The oxidised glass appears a transparent blue due to a measurable percentage of its copper as Cu^{2+}. Its visible spectrum is dominated by a weak, broad peak occurring at about 750 nm. These latter two glasses (containing Cu^{2+} and/or Cu^+) are optically clear for Raman scattering, and their Raman spectra should not be sensitive to the laser energy used for this study.

Decreasing the copper content from 0.25 wt% to 0.20 wt% leads to a proportional decrease in the 570 nm absorption, although the broad 430 nm absorption remains the same, as shown in Figure 2. A europium addition of 0.1 wt% shifts the narrow $(Cu^0)_n$ peak to about 590 nm, enhances the intensity of the absorbance, and eliminates the broad 430 nm component from the spectrum. The increase in absorbance is expected, as europium as Eu^{2+} reduces some of the Cu^+ to Cu^0 (which is then incorporated into the copper nanocrystals). The shift in peak location to higher wavelengths might be due to the formation of larger copper nanocrystals, that is an increase of "n" in $(Cu^0)_n$, in the presence of europium. However, as shown in Figure 2, a higher europium addition (0.4 wt% Eu) decreases and broadens the $(Cu^0)_n$ absorption, and unexpectedly yields a glass that is red in absorbed light but blue in transmitted light. This dichroism is assigned to the unique size and size distribution of nanocrystals dispersed in the glass [27].

3.2. Raman Signatures

A comparison of the Raman signatures for the copper-containing glasses is shown in Figure 3. The signature for the red $(Cu^0)_n$ glass is quite different than those for the transparent ones with

ionic copper, whatever the used excitation. The spectrum of light blue Cu^{2+} glass shows two principal peaks, a strong one at about 495 cm^{-1} with a shoulder around 575 cm^{-1} and a medium one at about 1015 cm^{-1}. The former peak is assigned to the Si-O bending envelope (using SiO_4 units as vibrational entities) [19-22] and the latter to the Si-O stretching envelope. The different spectral components (Q_n for stretching components, Q_n' for bending ones) of the above mentioned envelopes were assigned in the literature [19-22] to the vibrations of SiO_4 tetrahedra constituting the glass network : tetrahedron with zero (Q_0 or monomer, i.e. isolated SiO_4, ca. 750-850cm^{-1}), one (Q_1 or Si_2O_7 groups, ca. 950cm^{-1}), two (Q_2 or silicate chains, ca. 1000-1100cm^{-1}), three (Q_3 or sheet-like region, ca. 1100cm^{-1}) and four (Q_4, SiO_2 and tectosilicates, ca. 1150-1200cm^{-1}) bridging oxygen atoms (respectively four, three, two, one or zero non-bridging oxygen atoms) per silica tetrahedral structure group. The index of polymerization (I_p) calculated as the ratio of the bending to stretching Si-O areas [21,22] is close to 2 (see further discussion and Table 1). On the other hand, the Raman signature of red glass shows two peaks of rather similar intensity, which indicates a lower index of polymerization (~1), at 565 and 1075 cm^{-1}. A shoulder at 625 cm^{-1} and a (double) weak bump at about 910 cm^{-1} are also present. The spectrum is very similar to that observed for the glasses which have Na as main fluxing element. The SRL-131 glass is thus well representative of mold-blown ancient glass. Note that we do not see any evidence of Cu_2O or CuO Raman signatures (main peaks at respectively ~220 and 280-300, 345 and 632 cm^{-1} [13,28-29]), except the rather narrow component observed at ~625 cm^{-1} for Cu^0-containing glass. We think that this component does not correspond to copper oxide signature (see further discussion). The weak bump at ~1250cm^{-1} is associated to the BO_3 entities present in the glass network [22]. Assignment of the narrow peaks at ~1300 and 1440 cm^{-1} is not obvious (fig.5). Such doublet is expected for hexagonal BN.

Rather similar Raman signatures are observed for 0.20 wt% Cu-containing compositions (Fig. 4b). Under green excitation the fluorescence of the europium ion dominates the Raman spectrum and hinders an unambiguous measurement of the glass properties (as shown in Figure 5) because of such overlapping fluorescence phenomenon. Signature modification is, however, obvious: increase of the ~900cm^{-1} component, wavenumber shift of the Si-O stretching maximum to 1065 cm^{-1}, etc.

A very strong Rayleigh wing is also evident for Cu^0-containing glasses under blue excitation (Fig. 4), according to the broad spectral absorption assigned to isolated Cu^0 moieties (Fig. 1). The signatures due to SiO_4 framework are however distinguishable and rather similar to those given in Fig. 3: Cu^+-containing glass spectrum is similar to that of Cu^{2+}-containing glass under 532 nm excitation (main bumps at ~490 and 1015 cm^{-1}); on the other hand, Cu^0-containing glasses spectra have main bumps at 580-630 and 1080 cm^{-1}. A 250-300 cm^{-1} weak feature is also visible. Representative spectra recorded under red excitation are given in Fig. 6 for luster ceramics. As previously observed [7] the spectrum exhibits a very strong Rayleigh wing. In some places, we have succeeded in recording a ~25 cm^{-1} peak superimposed on the wing.

4. DISCUSSION

Different Raman signatures involve different silicate networks around the origin (focused light spot in the copper ion- or nanocrystal-containing glass) of the Raman scattering. Two rationales for why the Raman signature of the silicate network around the copper nanocrystal differs may be considered:

i) Because of the strong absorption in the energy range of the laser wavelength, the penetration depth of the laser beam is strongly decreased (typically the penetration depth decreases to a few tens of nanometer in heavy colored sample [30,31]) and the Raman signature of the red $(Cu^0)_n$ samples is essentially a surface phenomenon.

ii) The $(Cu^0)_n$ (or Cu^0) chromophore at the origin of the absorption interacts with the exciting laser line, resulting in a more-or-less resonant spectrum. The resonance Raman signature only involves the SiO_4 tetrahedra chemically bonded to the chromophore.

The Raman signature of the red glasses containing $(Cu^0)_n$ does not change significantly under blue excitation with chromophore content. For example, the Raman signatures of the red glasses with different copper contents as well as with different europium contents do not differ in the spectral range of the silicate network signature (100-1200 cm^{-1}), as shown by Figure 4b, even though their visible absorptions differ. This eliminates the first possible rationale; and accordingly, we can assign the difference in the Raman signature to the second explanation.

The Raman spectra of amorphous silicate provide information on the SiO_4 network arrangement through the band intensity and wavenumber. The strong intensity of the Si-O bending envelope at about 495 cm^{-1} in the Raman signature of the light blue glass indicates a highly polymerized SiO_4 network, as observed in many alkali silicate glasses and glazes processed at medium temperature [21,32]. On the contrary, the Raman spectra of red $(Cu^0)_n$-containing glasses with bumps of similar intensity, shifted to ~550 and 1080 cm^{-1}, are very similar to those of less polymerized glasses associated with centuries-old artifacts alkali silicate glass processed at lower temperature [32]). This indicates that the SiO_4 network in the vicinity of copper nanocrystals is different from the bulk matrix : metallic moieties induce the formation of a dual structure associating “isolated” Q_1 and well-polymerised (Q_3-Q_4) entities in the place of the medium connected pristine network. Consequently a lower index of polymerization is measured (Table 1). Main Qn/Qn’ components have been extracted using the procedure previously described [21,22] and representative fits are shown in Fig.7; mean values are listed in Table 1.

An unexpectedly strong Rayleigh “wing” is observed with the blue excitation, both for red $(Cu^0)_n$-containing glass and for the colorless Cu^+-containing glass. Such strong scattering could arise from

i) a “true” Rayleigh scattering due to a strong heterogeneity, which can be attributed to either dielectric or density heterogeneities. This behavior is understandable for red glasses with a dispersion of $(Cu^0)_n$ nanocrystals and of isolated Cu^0 atoms in the glass, both absorbing in the blue region. However, this is unexpected for Cu^+-containing glasses, unless these glasses also contain some copper nanocrystals and that these traces determine the Rayleigh (and Raman) signatures.

ii) the strong low wavenumber scattering could also arise from unresolved, damped, low wavenumber modes as expected for M^{n+} ions (or $(M^{n+})_m$ aggregates) [7] or for $(M^0)_n$ moieties [15-18]. In some places, we have succeeded in recording a spectrum with a ~30 cm^{-1} peak (Fig. 7). Any other Raman signature was obtained using red excitation on red-colored samples. Such signature is similar –except the downshifted wavenumber assigned to a mass effect, as expected-, to those recorded on $Ag^0(Ag^+)$-$Cu^0(Cu^+)$-containing luster ceramics (peaks at 45 and 65 cm^{-1} according the considered sample and/or orientation). Because of the higher Z number for Ag, the

Raman signature of Ag moieties (Ag^0 clusters or Ag^+ ions) is expected much more strong than that of Cu moieties [7].

That the silicate network has a diminished polymerization around a copper nanocrystal than around a copper ion is probably evidence that the $(Cu^0)_n$ particle disrupts its surrounding glass-forming structure. In essence, the silicate network must form a suitably-sized void to accommodate the $(Cu^0)_n$ nanocrystal, or conversely the colloidal particle must carve out a sufficiently large space within the network. Either way, the silicate network is broken up or de-polymerized around the $(Cu^0)_n$ nanocrystal.

5. CONCLUSIONS

Copper nanocrystals are formed during processing of the glass-forming melt under reduced atmospheres and are colloidally dispersed throughout the resulting red glass. Europium additions to the $(Cu^0)_n$-containing melt create nanocrystals that result in a dichroic glass. Convenient choice of the excitation wavelength gives a more-or-less resonance Raman spectrum and provides information on the Cu^0 moieties' environment. Green excitation appears a very sensitive probe to compare different glasses. The silicate network around a copper nanocrystal, $(Cu^0)_n$, in a glass is less polymerized than that around a copper ion, whether Cu^{2+} or Cu^+. This very preliminary investigation deserves further Raman studies versus exciting wavelength, especially in the green to infra-red range. The measurement of the (polarized) Raman cross-section versus exciting wavelength as a function of the M^0 content and its comparison with UV-visible absorbance curve may be useful in the future for further understanding of the lustre ceramics and glasses.

6. ACKNOWDLEGMENTS

G. Sagon is acknowledged for his technical help during this work and Mrs A. Tournier contribution in the data processing.

REFERENCES

1. Hornyak GL, Patrissi CJ, Oberhauser EB, Martin CR, Valmette JC, Lemaire L, Dutta J, Hofman H. *Nanostructured Materials* 1997; **9**: 571.
2. Barber D.J., Freestone I.C., *Archaeometry* 1990; **32**:33.
3. Bertan H, *Nouveau Manuel Complet de la Peinture sur Verre, sur Porcelaine et sur Email*, Encyclopédie-Roret, Mulo L Ed., Paris, 1913.
4. Carboni S, Glass from Islamic Lands, Thames & Hudson, London 2001.
5. Caiger-Smith A. *Luster Pottery – Technique, Tradition and Innovation in the Islam and the Western Worlds*, London, Faber & Faber, 1983.
6. Colomban Ph. *La Revue de la Ceramique et du Verre* 2004; **139**: 13.
7. Colomban Ph, Truong C. *J. Raman Sprectrosc.* 2004; **35**: 195.
8. Pérez-Arantegui J, Molera J, Larrea A, Pradell T, Vendrell-Saz M, Borgia I, Brunetti BG, Cariati F, Fermo P, Mellini M, Sgamellotti A, Viti C. *J. Amer. Ceram. Soc.* 2001; **84**: 442.
9. Padovani S, Sada C, Mazzoldi P, Brunetti BG, Borgia I, Sgamellotti A, Giulivi A, d'Acapito F, Battaglin G. *J. Appl. Phys.* 2003; **93**: 10058.
10. Padeletti G, Fermo P. *Appl. Phys*. 2004; **A79**: 241.
11. Fredrickx P, Hélary D, Schryvers D, Darque-Ceretti E. *Appl. Phys.* 2004; **A79**: 283.
12. Berthier S, Chevalley C, *La Couleur, Dossier Pour la Science*, 2000; **4**:22.
13. Pérez-Robles F, Garcia-Rodriguez FJ, Jimenez-Sandoval S, Gonzalez-Hernandez J. *J. Raman Spetrosc.* 1999; **30**: 1099.
14. Colomban Ph, Vendange V. *Sol-gel routes towards magnetic nanocomposites with tailored microwave absorption*, in *Proc. MRS Fall Meeting, 1^{srt}-6th December 1996, Boston, V-Nanophase and Nanocomposite Materials II*, Komarnemi S, Parker JC, Wollenberger HJ Eds. 1997; **457**: 451.
15. Qiu J, Shirai M, Nakaya T, Si J, Jiang X, Zhu C, Hirao K. *Appl. Phys. Lett*. 2002; **81**: 3040.
16. Ferrari M, Gonella F, Montagna M, Tosello C. *J. Appl. Phys*. 1996; **79**: 2055.
17. Gangopadhyay P, Kesavamoorthy R, Nair KGM, Dhandapani R. *J. Appl. Phys*. 2000; **88**: 4975.
18. De G, Tapfer L, Catalano M, Battaglin G, Caccavale, Gonella F, Mazzoldi P, Haglund RF Jr. *Appl. Phys. Lett*. 1996; **68**: 3820.
19. Mysen BO, Virgo D, Scarfe C. *Am. Mineral*. 1980; **65**: 690.
20. Seifert F, Mysen BO, Virgo D. *Am. Mineral*. 1982; **67**: 696.
21. Colomban Ph. *J. Non-Crystalline Solids* 2003; **323**: 180.
22. Colomban Ph, Treppoz F,. *J. Raman Sprectrosc.* 2001; **32**: 93.
23. Schreiber HD, Hockman AL. *J. Amer. Ceram. Soc.* 1987; **70**: 591.
24. Schreiber HD, Stokes ME. *The Glass Researcher* 2001; **11**: 13.
25. Morgan AB, Schreiber HD. *Ceram. Transactions* 1994; **45**: 145.
26. Schreiber HD, Stokes ME, Swink AM. *Ceram. Transactions* 2004; **141**: 315.
27. Edgar A. *J. Non-Crystalline Solids* 1997; **220**: 78.
28. Chrzanowski J, Irwin JC, *Solid State Communication* 1989; **70**: 11.

29. Irwin JC, Wei T, Franck J, *J. Phys.: Condens. Matter* 1991; **3**: 299.
30. Colomban Ph, Gouadec G, Mazerolles L. *Materials and Corrosion*. 2002; **53:** 306.
31. Derst G, Wilbertz C, Bhatia KL, Krätschmer W, Kalbitzer S, *Appl. Phys. Lett*. 1989; **54**: 1722.
32. Colomban Ph, March G, Mazerolles L, Karmous T, Ayed N, Ennabli A, Slim H. *J. Raman Spectrosc*. 2003; **34**: 205.

FIGURE CAPTIONS

Table 1: Q_n and Q_n' wavenumbers (in cm^{-1}) of Cu^0-, Cu^+- and Cu^{2+}-containing SRL-131 glass measured under different exciting laser lines. The index of polymerization (I_p) is given.

Figure 1: Visible absorption spectra for red (Cu^0), colorless (Cu^+), and light-blue (Cu^{2+}) glasses (sample photos are given to show the colour density) equilibrated at 1150°C under different oxygen fugacities; total copper content = 0.25 wt%. Blue, greens and red used excitation laser lines are drawn.

Figure 2: Visible absorption spectra for red (0.0 and 0.1 wt% Eu) and dichroic (0.4 wt% Eu) glasses equilibrated at 1150°C under reducing conditions; total copper content = 0.20 wt%. Used excitation laser lines are shown.

Figure 3: Representative Raman signatures of light-blue (Cu^{2+}) and red (Cu^0) glass for different exciting energy recorded in backscattering configuration. Detail of the low wavenumber range spectrum recorded with the high resolution XY instrument is given for red, colorless (Cu^+) and light-blue samples.

Figure 4: (a) Raman signatures of 0.25 wt% Cu colorless (Cu^+) and red (Cu^0) glass (blue and red excitations); (b) comparison with 0.2 wt% Cu red samples with different Eu doping.

Figure 5: Raman and Eu $^{2+}$-fluorescence signature of Eu doped Cu-containing SRL-131 glass under green excitation.

Figure 6 : Comparison of the low wavenumber region under 647.1 nm excitation for Cu^0/Ag^0-containing glasses: 0.25 wt% Cu SRL-131 glass recorded in different place, luster ceramic from Fustat (Fatimid, ~ 11th century) and from Suse (Abbasid, ~9th century).

Figure 7 : Q_n/Q_n' components of the bending (~500cm^{-1}) and stretching (1000cm^{-1}) Si-O modes are exampled for representative spectra of Cu^{2+} - and Cu^0-containing SRL-131 glasses.

Table 1

Q_n and Q_n' wavenumbers (in cm^{-1}) of Cu^0-, Cu^+- and Cu^{2+}-containing SRL-131 glass measured under different exciting laser lines. The index of polymerization (I_p) is given.

Q	Cu^{2+} / 532nm	Cu^+-Cu° / 488nm	Cu° / 532nm
Q_0	739,w		
Q_1	908w	897m	890m
Q_2	985S	950w;1000S	947w;985m
Q_3-Q_4	1056S	1078m	1075,vS; 1142w
Q_4			
Q_3'-Q_4'	430S	455m	515m
Q_2'	498w	490m	579S
Q_1'	578w	575vw	630w;670m
Q_0'			
I_p	1.9		0.8-1.2

S : strong, m : medium, w : weak, v : very.

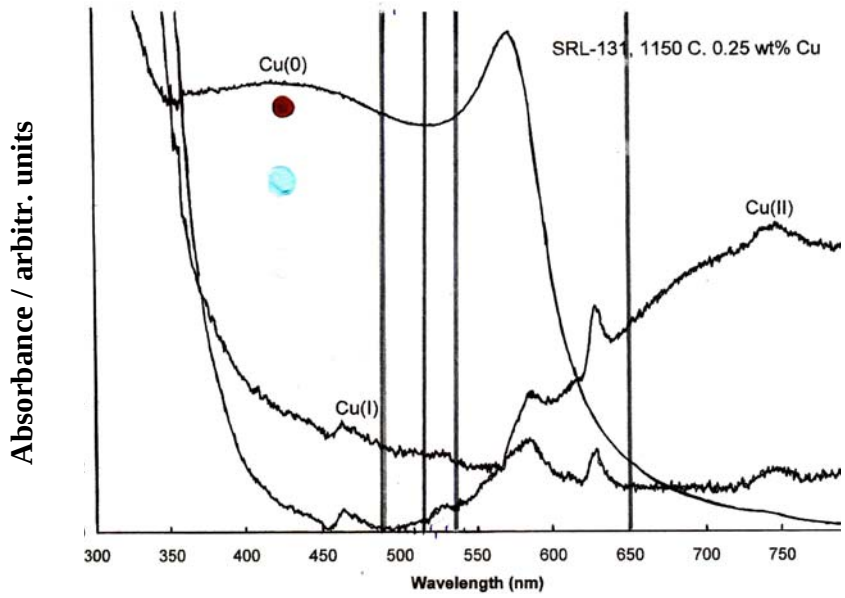

Figure 1: Visible absorption spectra for red (Cu^0), colorless (Cu^+), and light-blue (Cu^{2+}) glasses (sample photos are given to show the colour density) equilibrated at 1150°C under different oxygen fugacities; total copper content = 0.25 wt%. Blue, greens and red used excitation laser lines are drawn.

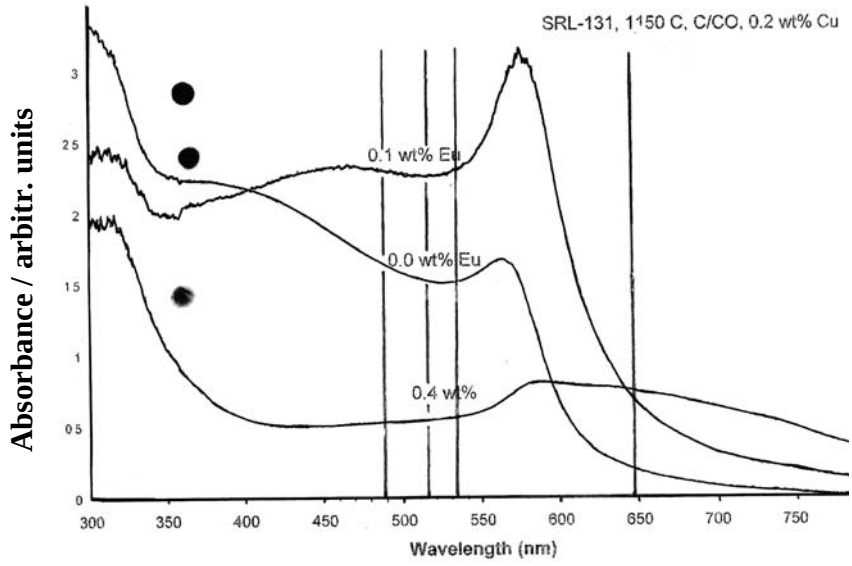

Figure 2: Visible absorption spectra for red (0.0 and 0.1 wt% Eu) and dichroic (0.4 wt% Eu) glasses equilibrated at 1150°C under reducing conditions; total copper content = 0.20 wt%. Used excitation laser lines are shown.

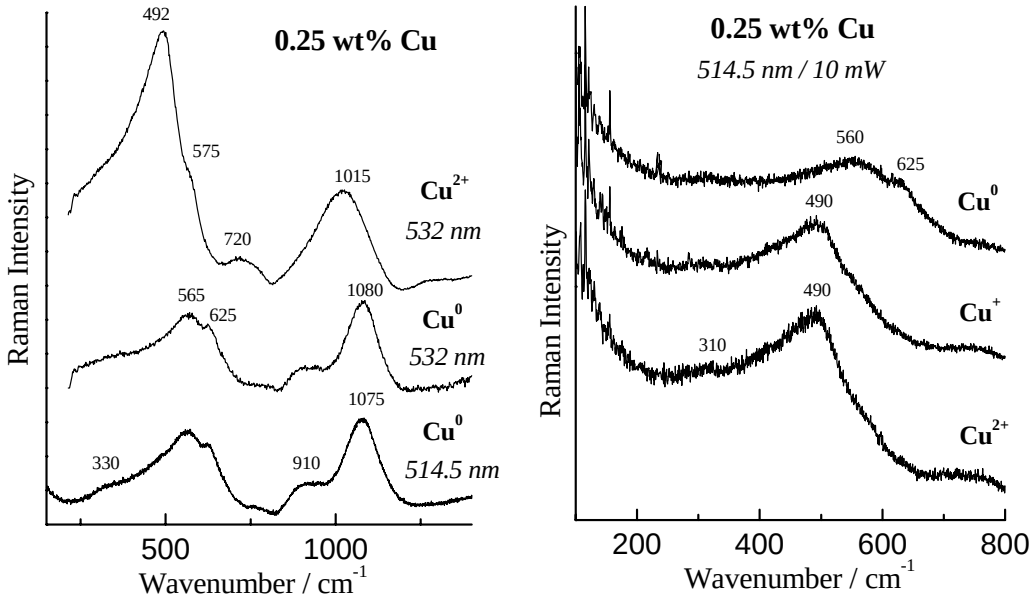

Figure 3: Representative Raman signatures of light-blue (Cu^{2+}) and red (Cu^{0}) glass for different exciting energy recorded in backscattering configuration. Detail of the low wavenumber range spectrum recorded with the high resolution XY instrument is given for red, colorless (Cu^{+}) and light-blue samples.

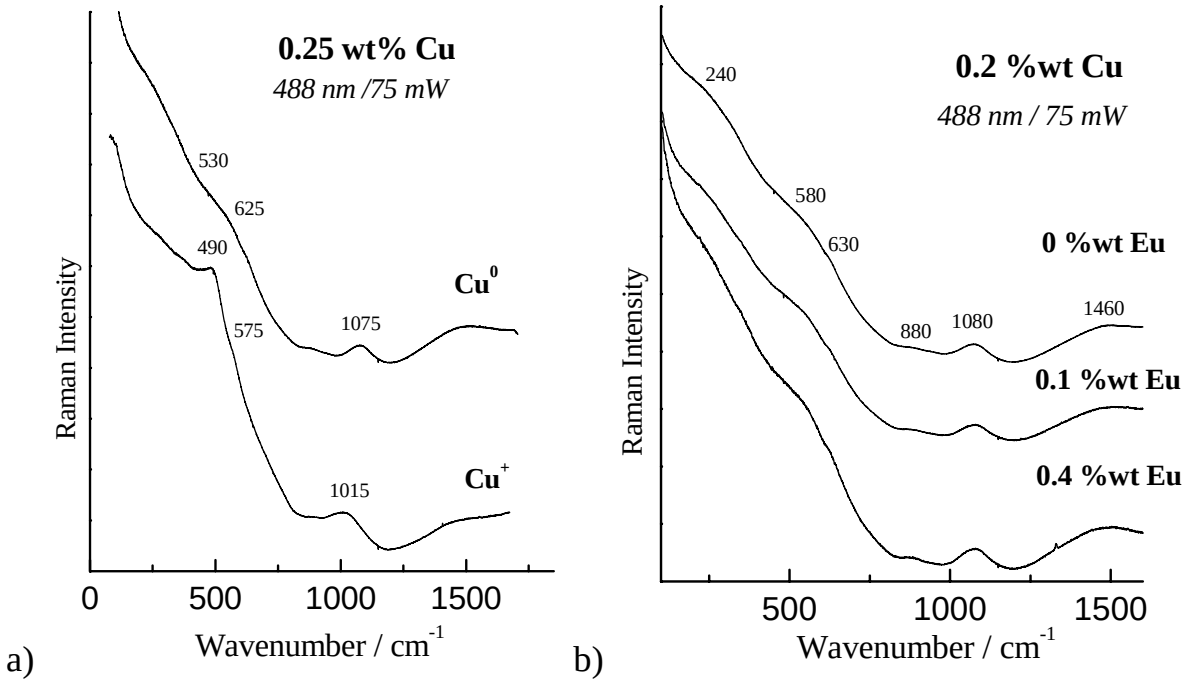

Figure 4: (a) Raman signatures of 0.25 wt% Cu colorless (Cu^{+}) and red (Cu^{0}) glass (blue and red excitations); (b) comparison with 0.2 wt% Cu red samples with different Eu doping.

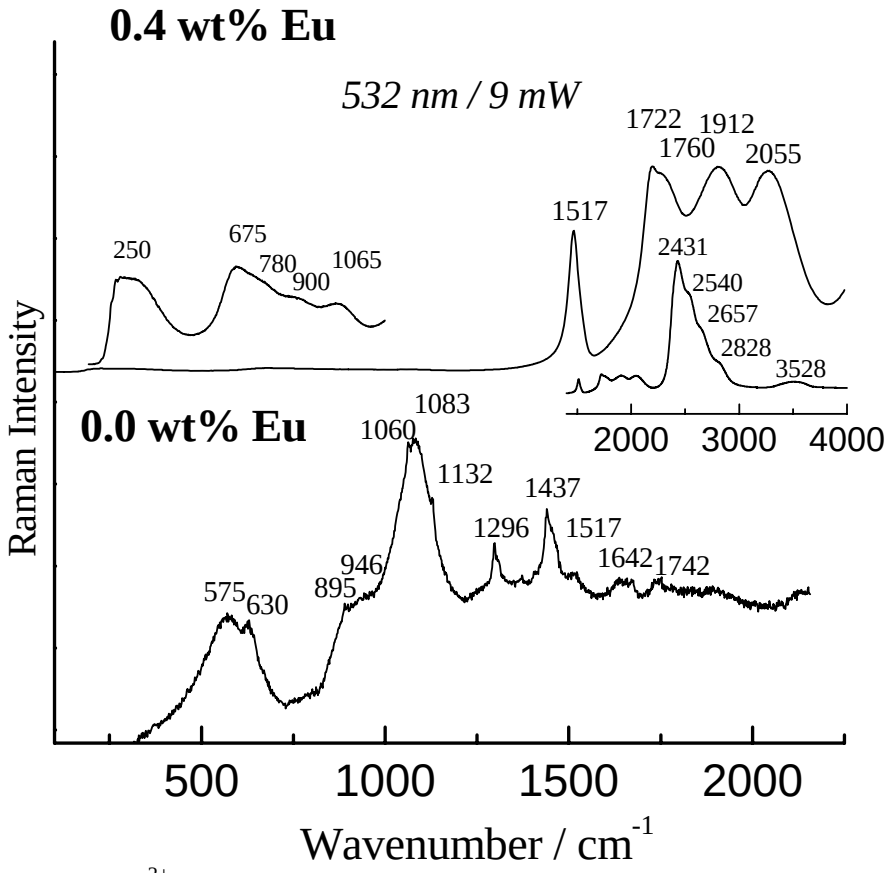

Figure 5: Raman and Eu $^{2+}$-fluorescence signature of Eu doped Cu-containing SRL-131 glass under green excitation.

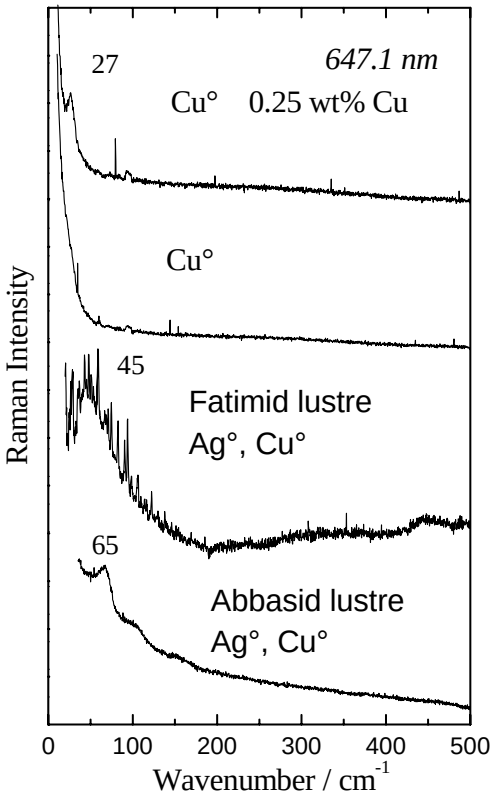

Figure 6 : Comparison of the low wavenumber region under 647.1 nm excitation for Cu^0/Ag^0-containing glasses: 0.25 wt% Cu SRL-131 glass recorded in different place, luster ceramic from Fustat (Fatimid, ~ 11^{th} century) and from Suse (Abbasid, ~9^{th} century).

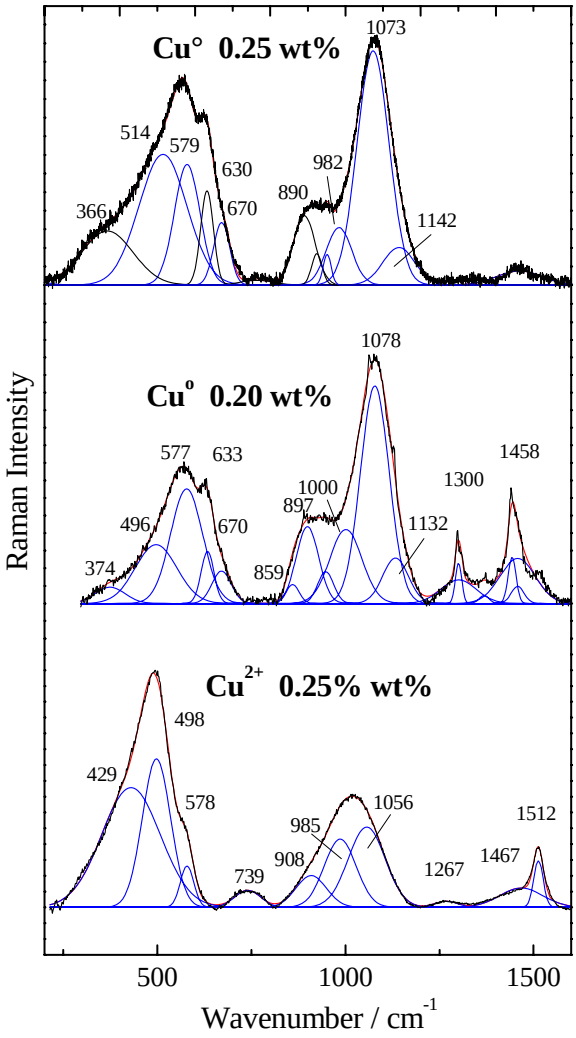

Figure 7 : Q_n/Q_n' components of the bending (~500cm^{-1}) and stretching (1000cm^{-1}) Si-O modes are exampled for representative spectra of Cu^{2+} - and Cu^0-containing SRL-131 glasses.